nature biotechnology

BRIEF COMMUNICATION

https://doi.org/10.1038/s41587-020-00794-3

Check for updates

Super-resolution RNA imaging using a rhodamine-binding aptamer with fast exchange kinetics

Murat Sunbul[1]✉, Jens Lackner[2], Annabell Martin[1], Daniel Englert[1], Benjamin Hacene[2], Franziska Grün[1], Karin Nienhaus[2], G. Ulrich Nienhaus[2,3,4,5]✉ and Andres Jäschke[1]✉

Overcoming limitations of previous fluorescent light-up RNA aptamers for super-resolution imaging, we present RhoBAST, an aptamer that binds a fluorogenic rhodamine dye with fast association and dissociation kinetics. Its intermittent fluorescence emission enables single-molecule localization microscopy with a resolution not limited by photobleaching. We use RhoBAST to image subcellular structures of RNA in live and fixed cells with about 10-nm localization precision and a high signal-to-noise ratio.

Super-resolution fluorescence microscopy of cellular structures continually provides fundamentally new insights into biology[1]. Over the years, an elaborate toolbox has become available to attach fluorescent markers to proteins for such studies. By contrast, marker tools for super-resolution RNA imaging are still scarce[2]. Recently, fluorescent light-up aptamers (FLAPs) have been recognized as promising tools for RNA imaging[3]. So far, they have mostly been employed for conventional, diffraction-limited imaging. FLAPs for super-resolution imaging were reported only last year, specifically the SiRA aptamer[4] for stimulated emission depletion (STED) microscopy and the Pepper aptamer[5] for structured illumination microscopy (SIM). Further optimization of these RNA markers will facilitate their widespread use in super-resolution microscopy.

Our laboratory has developed FLAPs that bind fluorophore–quencher conjugates and, thereby, disrupt contact quenching (Fig. 1a)[6,7]. This strategy affords the use of bright and photostable state-of-the-art fluorophores for RNA imaging[7,8]. For example, the SRB-2 aptamer binds various membrane-permeable rhodamine dyes with high affinity, but it does not provide sufficient sensitivity for imaging RNAs of low abundance in cells[9]. Here we present RhoBAST (Fig. 1b), a FLAP endowed with excellent photophysical properties that were optimized for single-molecule localization microscopy (SMLM)[10]. With this technique, we have visualized subnuclear RNA structures in live and fixed cells with image resolutions far beyond the classical diffraction limit.

Starting from a 15% doped SRB-2 aptamer library, in vitro evolution was employed to improve the affinity, thermal stability, photostability and brightness of SRB-2 using tetramethylrhodamine (TMR) as bait (Fig. 1c,d). After incubation of the library with TMR-decorated beads, mutants binding TMR were specifically eluted, amplified and subsequently used as input for the next round of evolution. Enrichment of the library was confirmed by the fractional increase of eluted RNA and the fluorescence enhancement of the fluorophore–quencher conjugate TMR-dinitroaniline (TMR-DN) upon mixing with RNA pools after each round (Fig. 1d). After seven iterations, the enriched variants were sequenced and screened for fluorescence enhancement upon binding TMR-DN (Supplementary Fig. 1). Sequence and truncation analysis (Supplementary Figs. 2 and 3) revealed two beneficial mutations in the SRB-2 sequence, namely an insertion of a single U nucleotide between C6 and U7 and a U22A mutation (Supplementary Fig. 4). These features were incorporated into the design of SRB-3 (Supplementary Fig. 4), which exhibits 50% higher brightness and 1.8-fold higher affinity ($K_D = 20 \pm 1$ nM) for TMR-DN than SRB-2. To eliminate alternative secondary structures predicted for SRB-3 (Supplementary Fig. 5), we rationally exchanged the U8-A19 base pair by C-G and the UUCG tetraloop by GAAA (Fig. 1b). Indeed, these mutations were beneficial, resulting in a new aptamer dubbed RhoBAST (Rhodamine Binding Aptamer for Super-resolution Imaging Techniques). It features a fraction of $86 \pm 5\%$ in the proper fold, a 26-fold fluorescence turn-on and a K_D of 15 ± 1 nM (Supplementary Fig. 6).

SRB-2, SRB-3 and RhoBAST have similar circular dichroism (CD) spectra (Supplementary Fig. 6). The fluorescence emission of their complexes with TMR-DN is independent of sodium or potassium ions but strictly depends on the magnesium ion (Mg^{2+}) concentration (Supplementary Fig. 7), in contrast to G-quadruplex-forming FLAPs[11–13]. However, RhoBAST:TMR-DN retains more than 90% of its maximum fluorescence at 0.25 mM Mg^{2+}, implying that RhoBAST functions effectively under physiological conditions (Supplementary Fig. 7). RhoBAST:TMR-DN exhibits excellent brightness and well-defined fluorescence spectra, with excitation and emission maxima at 564 nm and 590 nm, respectively (Fig. 1e). It is 4.6- and 7.6-fold brighter than Broccoli:DFHBI-1T[11] and Corn:DFHO[12], respectively, and has similar brightness to Pepper:HBC620 (Pepper620)[5], which is the brightest and most photostable version of Pepper aptamer:dye complexes (Supplementary Table 1). With a melting point, T_m, of 79 °C, RhoBAST is extremely thermostable. Consequently, upon raising the temperature to 37 °C, RhoBAST:TMR-DN retains 69% of its fluorescence intensity at 25 °C, compared to 54% for SRB-2:TMR-DN (Supplementary Fig. 6). Furthermore, RhoBAST:TMR-DN appears remarkably photostable. Only 1% of its fluorescence was bleached during 3 h of continuous

[1]Institute of Pharmacy and Molecular Biotechnology (IPMB), Heidelberg University, Heidelberg, Germany. [2]Institute of Applied Physics (APH), Karlsruhe Institute of Technology (KIT), Karlsruhe, Germany. [3]Institute of Nanotechnology (INT), Karlsruhe Institute of Technology (KIT), Eggenstein-Leopoldshafen, Germany. [4]Institute of Biological and Chemical Systems (IBCS), Karlsruhe Institute of Technology (KIT), Eggenstein-Leopoldshafen, Germany. [5]Department of Physics, University of Illinois at Urbana–Champaign, Urbana, IL, USA. ✉e-mail: msunbul@uni-heidelberg.de; uli.nienhaus@kit.edu; jaeschke@uni-hd.de

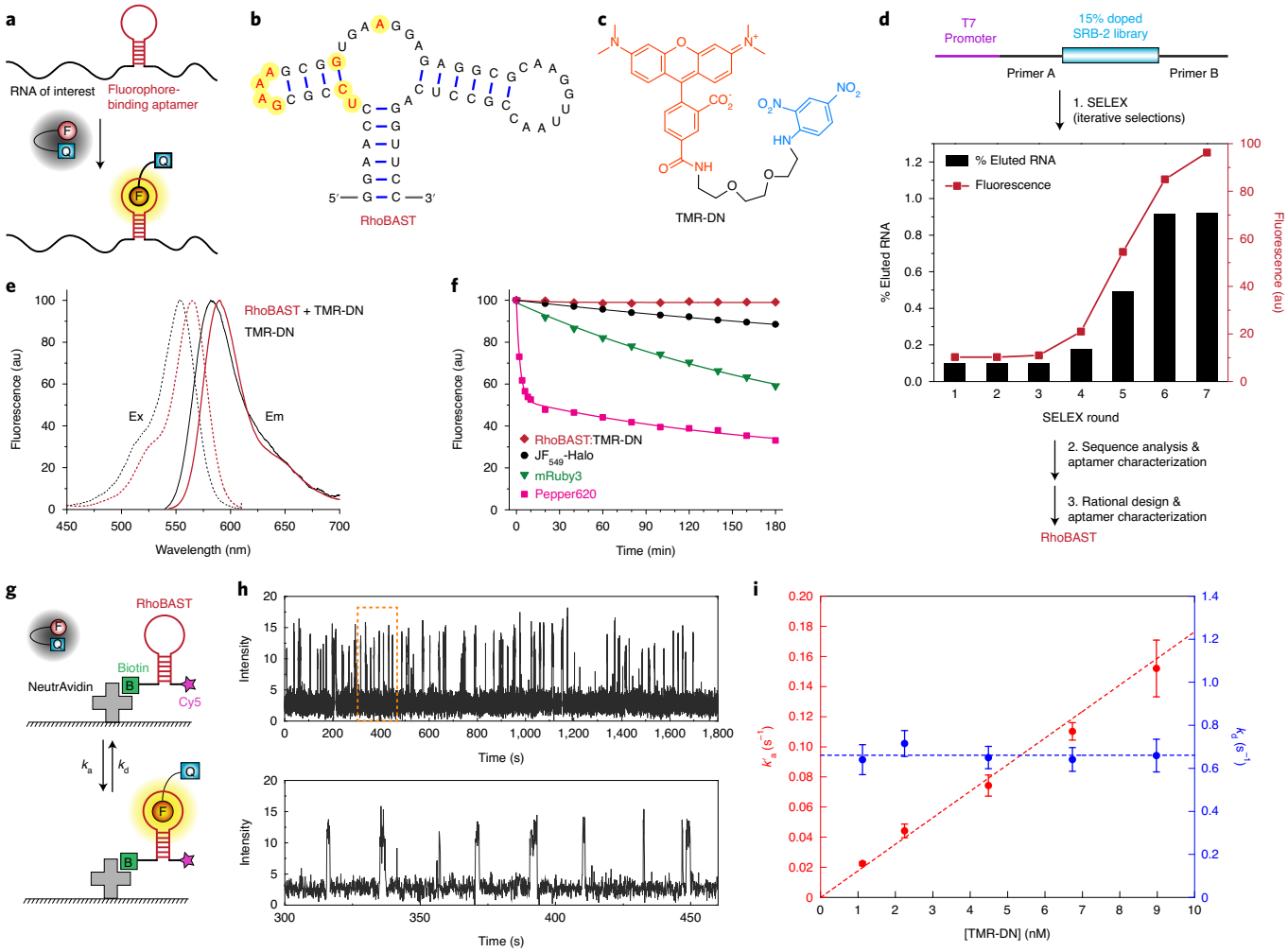

Fig. 1 | Directed evolution and characterization of RhoBAST. a, Scheme showing the genetically encoded fluorophore-binding aptamer and a contact-quenched fluorophore–quencher (F–Q) conjugate for imaging an RNA of interest. F–Q is non-fluorescent in solution and lights up upon binding to the aptamer. **b**, Predicted secondary structure of RhoBAST; changed ribonucleotides are highlighted in yellow. **c**, Chemical structure of TMR-DN. TMR, orange; polyethylene glycol linker, black; DN, blue. **d**, Directed evolution of RhoBAST for binding to the TMR fluorophore using iterative cycles of SELEX and rational design. The initial library was composed of 15% doped SRB-2 flanked by constant primer A and primer B binding regions. The T7 promoter was used for efficient transcription of the library by T7 RNA polymerase. Progress of selection was assessed by calculating the percentage of eluted RNA and the fluorescence enhancement of TMR-DN upon addition of RNA pools after each round. **e**, Normalized excitation and emission spectra of TMR-DN and RhoBAST:TMR-DN. **f**, Fluorescence intensity decay upon constant-level illumination of TMR-DN (20 nM) complexed with RhoBAST (500 nM), the JF_{549}-Halo fluorophore (20 nM), the fluorescent protein mRuby3 (20 nM) and HBC620 (20 nM) complexed with Pepper (500 nM). After 3 h, the fractional decrease was 1.0 ± 0.4%, 11.5 ± 0.9%, 40.0 ± 2.2% and 66.4 ± 2.2% (mean ± s.d., $n = 3$ independent experiments), respectively. **g**, Scheme showing on and off switching of the fluorescence due to TMR-DN association to and dissociation from RhoBAST immobilized on a coverslip. RhoBAST was modified with biotin at 5′ and Cy5 at 3′ and bound to the glass surface via NeutrAvidin. **h**, Top, fluorescence time trace taken on an individual, surface-immobilized RhoBAST molecule after addition of TMR-DN (2.2 nM) containing buffer. Bottom, expanded view of the time trace (300–460 s, marked by the dashed box), revealing multiple fluorescence bursts due to continuous TMR-DN association and dissociation. **i**, Dependence of the average dissociation ($k_d = <\tau_{on}>^{-1}$) and association ($k'_a = k_a c = <\tau_{off}>^{-1}$) rate coefficients on the TMR-DN concentration. Here, $<\tau_{on}>$ and $<\tau_{off}>$ are the average lengths of emissive and dark time periods, respectively. Data are shown as mean ± s.d. See Methods for further details on the statistical analysis.

illumination, whereas the rhodamine-based JF_{549}-Halo fluorophore, the mRuby3 fluorescent protein and Pepper620 decreased their fluorescence by 12%, 40% and 66%, respectively, under identical conditions (Fig. 1f and Supplementary Note 1).

Next, we measured the kinetic parameters of TMR-DN association to and dissociation from the aptamers using single-molecule imaging. To this end, RhoBAST molecules were sparsely immobilized on glass surfaces (Fig. 1g). After adding TMR-DN solution, fluorescence intensity time traces from individual molecules were acquired (Fig. 1h). Analysis of the fluorescence on and off times in these traces as a function of the TMR-DN concentration in the range of 1–10 nM yielded dissociation ($k_d = 0.66 \pm 0.01\ s^{-1}$) and association ($k_a = 1.8 \pm 0.1 \times 10^7\ M^{-1}s^{-1}$) rate coefficients (Fig. 1h,i), resulting in $K_D = 37 \pm 3$ nM, which agrees well with those of solution measurements (Supplementary Fig. 6 and Supplementary Note 2). A TMR-DN ligand remains bound to RhoBAST for 1.5 s on average, dissociates and is replaced by a new ligand within about 5 s (at 10 nM). Stopped-flow spectrometry on solutions also revealed more than 200- and 300-fold greater association and dissociation rates, respectively, for RhoBAST in comparison to other FLAPs

under the same conditions (Supplementary Note 2). Consequently, RhoBAST emission displays fast intermittency (blinking), which is a key requirement for SMLM. Continuous ligand exchange implies that the number of photons, N, captured from the aptamer is not limited by photobleaching. As the localization precision scales with $N^{-1/2}$, molecular positions can be determined with, in principle, unlimited precision. Ligand exchange also has been exploited by SMLM variants such as DNA-PAINT[14], but the light-up property of RhoBAST:TMR-DN is a clear additional advantage. These favorable characteristics make the RhoBAST:TMR-DN system a superb genetically encoded tag for RNA imaging in fixed and live cells using super-resolution SMLM as well as classical, diffraction-limited microscopy.

We evaluated RhoBAST in comparison to SRB-2 and SRB-3 for diffraction-limited confocal imaging of *Escherichia coli* bacteria. Single copies of the aptamers without stabilizing scaffolds were fused to the 3′ untranslated region (UTR) of green fluorescent protein (*gfp*) (Supplementary Fig. 8). In the TMR detection channel, the signal-to-background ratios for bacteria expressing *gfp-RhoBAST*, *gfp-SRB-3* and *gfp-SRB-2* messenger RNAs (mRNAs) were, respectively, 14 ± 1, 8 ± 1 and 4 ± 1. These values were calculated by dividing the average fluorescence intensity at the poles of bacteria expressing the *gfp-aptamer* by that of bacteria expressing only gfp mRNA (Supplementary Fig. 8). Moreover, the fluorescence intensity of RNAs carrying multiple RhoBAST repeats increased almost linearly up to eight repeats and still showed 70% of the expected value at 16 repeats (Supplementary Fig. 9). Such constructs with enhanced emission can greatly facilitate imaging of low-abundance RNAs. To analyze the sensitivity of RhoBAST:TMR-DN, bacteria expressing different amounts of *gfp-RhoBAST*$_{16}$ mRNA were fixed with paraformaldehyde (PFA) and imaged. Even at a level of ~1 molecule of *gfp-RhoBAST*$_{16}$ per cell (quantified by reverse transcription quantitative polymerase chain reaction (RT–qPCR)), significantly higher fluorescence was detected in the TMR channel than in control bacteria expressing only *gfp* mRNA (Supplementary Fig. 9). Furthermore, to image endogenously expressed mRNAs, multiple RhoBAST repeats were stably introduced into the genome of *E. coli* K12, and *ompA*, *rnaseE* and *cat* mRNAs displayed distinct localization patterns in the images (Supplementary Fig. 10).

To investigate RhoBAST:TMR-DN for optical microscopy of live mammalian cells, a diverse set of RNA species with different reported localization patterns and transcribed from different promoters were examined. First, RhoBAST embedded into the Tornado plasmid system[15] was expressed as a single-copy, circular aptamer under the control of the U6 promoter in HEK293T cells. Besides nuclear puncta, most of the circular RhoBAST was observed in the cytosol (Fig. 2a), as previously reported for circular Broccoli[15] and Corn[16]. This result shows that RhoBAST folds properly and functions as expected in mammalian cells. Second, *GFP* mRNA tagged with RhoBAST$_{16}$ was expressed under the CAG promoter in live HEK293T cells, revealing the typical cytosolic localization of *GFP* mRNA (Fig. 2b). Third, the CGG trinucleotide repeat-containing *FMR1* (fragile-X mental retardation gene)-*GFP* mRNA fused to RhoBAST$_{16}$ was expressed in HeLa cells under the CMV promoter. It showed the distinct nuclear aggregation pattern reported for this mRNA[17] (Fig. 2c). The low fluorescence in the TMR channel of control cells demonstrates the specific effect of RhoBAST on the TMR-DN fluorescence (Fig. 2d). Furthermore, when *GFP-RhoBAST*$_{16}$ mRNA was expressed at low levels in HeLa cells, we observed individual spots in the TMR channel, co-localizing with single-molecule fluorescence in situ hybridization (smFISH) probes that specifically hybridize to the GFP sequence (Fig. 2e,f). This experiment indicates that RhoBAST is still intact and functional after the smFISH protocol and highlights its sensitivity and specificity. Tagging RNAs of interest (ROIs) with RhoBAST did not change their localizations (Supplementary Fig. 11) and did not interfere with degradation by exonuclease XRN1 (Supplementary Fig. 12).

To assess RhoBAST:TMR-DN in super-resolution SMLM applications, we visualized *gfp-RhoBAST* mRNA in bacteria. Excellent super-resolution images were obtained (Fig. 2g) owing to the fast blinking (ligand exchange) of the RhoBAST:TMR-DN system, resolving even single aptamers. In contrast, SMLM imaging of *gfp-Pepper* with the HBC620 dye was severely compromised due to its slow dye exchange (Supplementary Fig. 13 and Supplementary Note 2) and fast fluorescence decay under illumination (Fig. 1f and Supplementary Video 1). Next, we imaged structures inside the cell nucleus formed upon expression of circular RhoBAST in live and fixed HEK293T cells. Intriguingly, we observed hollow spheres in the nucleus, details of which were hardly visible in the epifluorescence image (Fig. 2h and Supplementary Fig. 14). Elaborate immunofluorescence and co-localization studies of these subnuclear structures with literature-reported nuclear bodies (Supplementary Fig. 15) revealed that cyclic RhoBAST in the nucleus co-localized with NONO and PSPC1, proteins that are crucial components of paraspeckle nuclear bodies[18]. Presumably, the high concentration of circular RhoBAST in the nucleus triggers phase separation of RNA

Fig. 2 | Confocal, epifluorescence and SMLM with the RhoBAST:TMR-DN system. a, Confocal imaging of live HEK293T cells expressing circular RhoBAST aptamers transcribed under the control of the U6 promoter using the Tornado system. Cells were co-transfected with another GFP-expressing plasmid as a transfection control. **b**, Confocal imaging of live HEK293T cells expressing *GFP* mRNA fused to RhoBAST$_{16}$ transcribed under the control of CAG promoter. **c**, Confocal imaging of live HeLa cells expressing the trinucleotide CGG repeat-containing *FMR1-GFP* mRNA fused to RhoBAST$_{16}$ transcribed under the control of CMV promoter in HeLa cells. **d**, Confocal imaging of live HEK293T cells expressing GFP (negative control) to show the background fluorescence due to the presence of free TMR-DN. **e**, Comparison of *GFP-RhoBAST*$_{16}$ mRNA imaging using smFISH and RhoBAST:TMR-DN. *GFP-RhoBAST*$_{16}$ mRNAs in fixed HeLa cells were first hybridized to Atto647N-conjugated smFISH probes (specific to GFP sequence) and then incubated with TMR-DN and imaged. **f**, Scatter plot showing the co-localization of the TMR and smFISH channels in **e** (Pearson's coefficient = 0.856). **g**, Epifluorescence and SMLM images of *gfp-RhoBAST* mRNA in fixed *E. coli* bacteria. Fluorescence intensity profiles across the six dots marked by white arrows. Symbols, experimental data; thin lines, Gaussian fits to the individual profiles; thick line, Gaussian fit to the average profile, yielding a full width at half maximum (FWHM) of 73 ± 5 nm. The constant widths of the individual dots suggest that they represent single fluorophores. Additional support comes from the average localization uncertainty, $\sigma = 32 \pm 7$ nm, of the emitters in the SMLM map, which is consistent with the FWHM. **h**, Epifluorescence and SMLM images of live HEK293T cells showing hollow spheres containing circular RhoBAST in the nuclei. Fluorescence intensity profiles along the white lines show the effective background removal and the much higher spatial resolution of SMLM. Gaussian fitting yields FWHM values for the left and right peaks, respectively, of 77.8 ± 0.3 and 95.8 ± 0.7 nm in the SMLM profile, and 590 ± 10 and 750 ± 10 nm in the epifluorescence image, respectively. **i**, *tolB-gfp* mRNA fused to RhoBAST$_{16}$ in fixed bacteria was imaged via SMLM and epifluorescence. These images are also shown as overlays on top of bright-field images. **j**, Epifluorescence and SMLM images of the trinucleotide CGG repeat-containing *FMR1-GFP* mRNA fused to RhoBAST$_{16}$ in HeLa cells. **k**, Epifluorescence and SMLM images of HeLa cells expressing *GFP-RhoBAST*$_{16}$ mRNA labeled with Atto647N-conjugated smFISH probes (specific to the GFP sequence) and TMR-DN. The overlay image shows significant co-localization (in white). Scale bars in **a**–**e**, 10 µm; in **g**, 500 nm; in **h**, 4 µm (left) and 1 µm (middle, right), respectively; in **i**, 1 µm; in **j**, 4 µm and 1 µm, respectively; in **k**, 4 µm. At least three independent experiments were carried out with similar results.

with the assistance of NONO and PSPC1, forming paraspeckle-like nuclear bodies (Supplementary Fig. 16).

In SMLM, multiple RhoBAST repeats can increase the total number of association and dissociation events within a given time interval. Thus, the overall image acquisition time decreases, as photons can be collected at a higher rate to pinpoint the position of the target RNA. The larger tag size is of lesser concern unless one aims at very high image resolution (<10 nm). We imaged *tolB-gfp-RhoBAST*$_{16}$ mRNA in bacteria, where the TolB signal peptide should cause localization of the mRNA at the inner bacterial membrane due to signal recognition particle (SRP)-mediated co-translational translocation[19] of TolB-GFP. Indeed, it was possible to use fewer camera frames (shorter overall exposure time) to collect high-quality SMLM images, which clearly revealed that *tolB-gfp-RhoBAST*$_{16}$ mRNA localized at the inner membrane (Fig. 2i and Supplementary Figs. 17 and 18). In contrast, *gfp-RhoBAST*$_{16}$ lacking the tolB sequence or carrying another SRP-independent signal peptide sequence showed substantially different localization patterns (Supplementary Fig. 17). Localization of *tolB-gfp-RhoBAST*$_{16}$, *gfp-RhoBAST*$_{16}$ and *gfp* mRNAs was

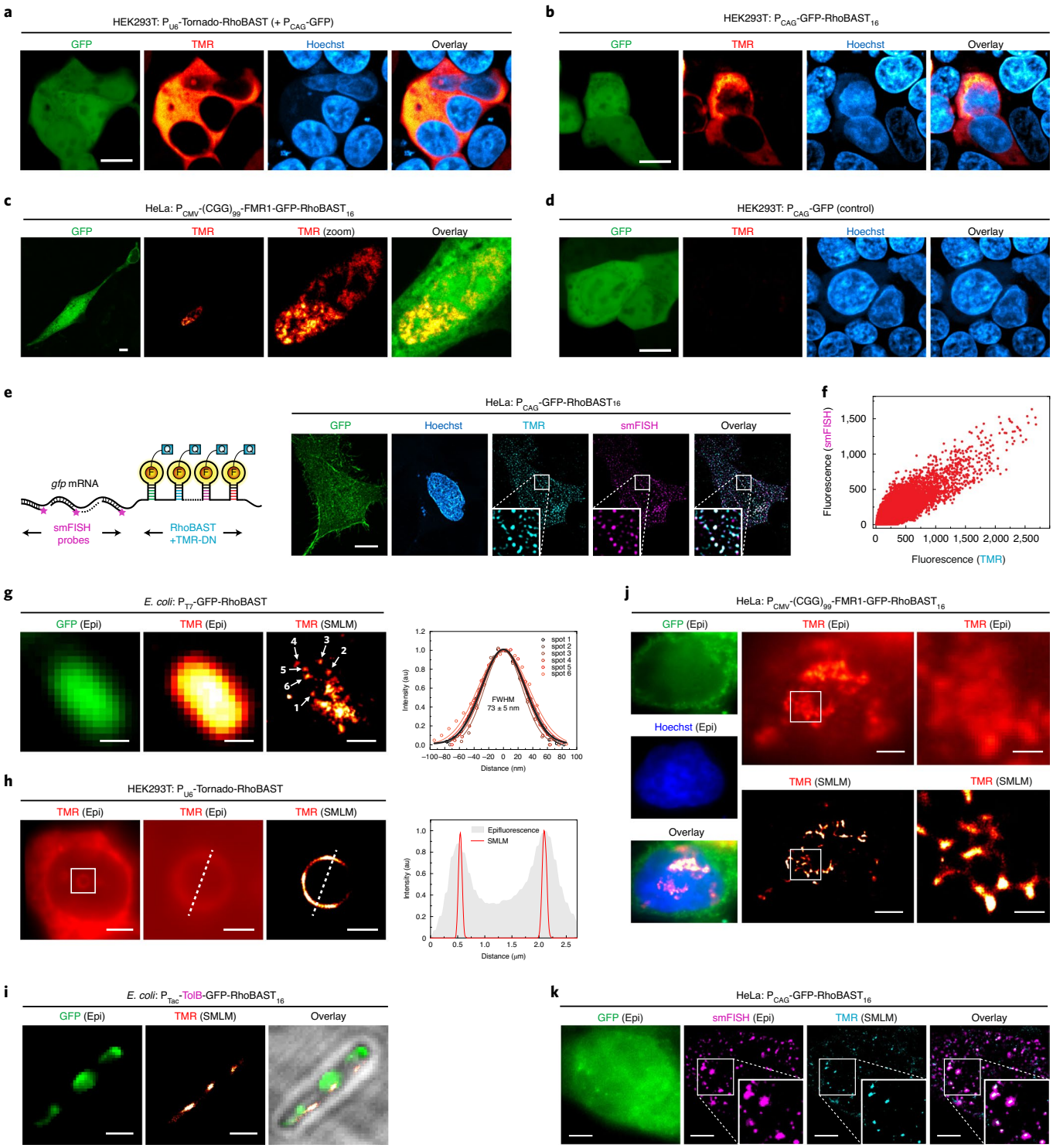

also validated by smFISH probes as well as super-resolution SIM[20] (Supplementary Figs. 19 and 20). Furthermore, we imaged $(CGG)_{99}$-*FMR1-GFP-RhoBAST*$_{16}$ mRNA in mammalian cells with SMLM to reveal architectural details of disease-causing RNA aggregates containing CGG repeats, which are excessively formed in patients with fragile X syndrome (Fig. 2j, Supplementary Fig. 21 and Supplementary Video 2). Finally, we explored dual-color microscopy of *GFP-RhoBAST*$_{16}$ mRNA expressed at low levels in HeLa cells using far-red fluorescent smFISH probes (specific to the GFP sequence) and TMR-DN. SMLM images in the TMR channel displayed a high degree of co-localization with epifluorescence images in the far-red channel (Fig. 2k). Note the much enhanced resolution of the SMLM image in the figure.

In summary, we have introduced a next-generation rhodamine-binding aptamer, RhoBAST, as a genetically encoded tag for super-resolution RNA imaging. The RhoBAST:TMR-DN system is the first FLAP that was specifically developed for live cell SMLM, owing to its continuous and fast fluorophore exchange combined with exceptionally high photostability and brightness. In comparison to its parent, SRB-2, it features markedly improved folding and thermal stability, higher affinity to TMR-DN as well as higher fluorescence quantum yield and photobleaching resistance. With RhoBAST:TMR-DN, subcellular and subnuclear structures of RNA can readily be visualized with excellent localization precision in live or fixed specimens.

Online content

Any methods, additional references, Nature Research reporting summaries, source data, extended data, supplementary information, acknowledgements, peer review information; details of author contributions and competing interests; and statements of data and code availability are available at https://doi.org/10.1038/s41587-020-00794-3.

Received: 15 March 2020; Accepted: 10 December 2020;
Published online: 11 February 2021

References

1. Sigal, Y. M., Zhou, R. & Zhuang, X. *Science* **361**, 880–887 (2018).
2. Schmidt, A., Gao, G., Little, S. R., Jalihal, A. P. & Walter, N. G. *Wiley Interdiscip. Rev. RNA* **11**, e1587 (2020).
3. Su, Y. & Hammond, M. C. *Curr. Opin. Biotechnol.* **63**, 157–166 (2020).
4. Wirth, R., Gao, P., Nienhaus, G. U., Sunbul, M. & Jäschke, A. *J. Am. Chem. Soc.* **141**, 7562 (2019).
5. Chen, X. et al. *Nat. Biotechnol.* **37**, 1287–1293 (2019).
6. Sunbul, M. & Jäschke, A. *Angew. Chem. Int. Ed.* **52**, 13401–13404 (2013).
7. Arora, A., Sunbul, M. & Jäschke, A. *Nucleic Acids Res.* **43**, e144 (2015).
8. Braselmann, E. et al. *Nat. Chem. Biol.* **14**, 964–971 (2018).
9. Sunbul, M. & Jäschke, A. *Nucleic Acids Res.* **46**, e110 (2018).
10. Li, Y., Ishitsuka, Y., Hedde, P. N. & Nienhaus, G. U. *ACS Nano* **7**, 5207–5214 (2013).
11. Filonov, G. S., Moon, J. D., Svensen, N. & Jaffrey, S. R. *J. Am. Chem. Soc.* **136**, 16299–16308 (2014).
12. Song, W. et al. *Nat. Chem. Biol.* **13**, 1187–1194 (2017).
13. Autour, A. et al. *Nat. Commun.* **9**, 656 (2018).
14. Schnitzbauer, J., Strauss, M. T., Schlichthaerle, T., Schueder, F. & Jungmann, R. *Nat. Protoc.* **12**, 1198–1228 (2017).
15. Litke, J. L. & Jaffrey, S. R. *Nat. Biotechnol.* **37**, 667–675 (2019).
16. Kim, H. & Jaffrey, S. R. *Cell Chem. Biol.* **26**, 1725–1731 e1726 (2019).
17. Hagerman, R. J. & Hagerman, P. *Nat. Rev. Neurol.* **12**, 403–412 (2016).
18. Fox, A. H., Nakagawa, S., Hirose, T. & Bond, C. S. *Trends Biochem. Sci.* **43**, 124–135 (2018).
19. Steinberg, R., Knupffer, L., Origi, A., Asti, R. & Koch, H. G. *FEMS Microbiol. Lett.* **365** (2018).
20. Wu, Y. & Shroff, H. *Nat. Methods* **15**, 1011–1019 (2018).

Methods

General. All reagents were purchased from Sigma-Aldrich or Thermo Fisher Scientific unless otherwise specified and used without further purification. Reverse-phase high-performance liquid chromatography purifications were performed on a Luna 5 µm C18(2) 100 Å column, 250 mm × 10 mm (Phenomenex), and compounds were eluted with a mixture of buffer A consisting of 100 mM Et_3N/AcOH (pH 7.0) in Milli-Q-water and buffer B containing 100 mM Et_3N/AcOH (pH 7.0) in an acetonitrile:water (4:1) mixture. High-resolution mass spectra were recorded on a Bruker microTOFQ-II ESI mass spectrometer. DNA and RNA concentrations were determined with a NanoDrop ND-1000 spectrophotometer (NanoDrop Technologies). Fluorescence measurements were performed with a JASCO FP-6500 spectrofluorometer equipped with an ETC-273T digital temperature controller. CD spectra were recorded on a JASCO J-810 spectropolarimeter. Stopped-flow experiments were conducted using an SX-18 M stopped-flow spectrometer (Applied Photophysics). Agarose gels were stained with ethidium bromide and visualized by ultraviolet (UV) illumination using an AlphaImager 2200 (Alpha Innotech). Absorbance spectra were recorded on a Cary 50 UV-Vis spectrophotometer (Varian). Synthetic DNA oligonucleotides were purchased from Integrated DNA Technologies (IDT). HEK293T cells (DSMZ, ACC 635) and HeLa cells (DSMZ, ACC 57) were cultured at 37 °C under 5% CO_2 in Dulbecco's Modified Eagle's Medium containing high glucose, HEPES and glutamine without phenol red (Thermo Fisher Scientific) supplemented with 10% FBS, 100 U ml^{-1} of penicillin and 100 µg ml^{-1} of streptomycin. *E. coli* DH5α, K12 and BL21 Star (DE3) cells (Thermo Fisher Scientific) were typically grown at 37 °C with shaking at 150 r.p.m. in Luria–Bertani (LB) medium.

Synthesis. Synthesis and characterization of TMR-SS-Biotin (used for systematic evolution of ligands by exponential enrichment (SELEX)) and TMR-DN are described in Supplementary Note 3.

DNA library preparation for SELEX. A 93-nucleotide-long single-stranded DNA (ssDNA) oligonucleotide library consisting of a 15% doped 54-nucleotide SRB-2 sequence flanked by two constant primer binding sites was synthesized (IDT). DNA library sequence (5′ to 3′):

GGAGCTCAGCCTTCACTGC(N3)(N3)(N1)(N1)(N2)(N2)(N4)(N2)(N3)(N2)(N4)(N4)(N2)(N3)(N3)(N2)(N3)(N1)(N4)(N3)(N1)(N4)(N3)(N3)(N1)(N3)(N1)(N3)(N3)(N2)(N3)(N2)(N1)(N1)(N3)(N3)(N4)(N4)(N1)(N1)(N2)(N2)(N3)(N2)(N2)(N4)(N2)(N1)(N3)(N3)(N4)(N4)(N2)(N2)GGCACCACGGTCGGATCCAC. N1, N2, N3 and N4 are mixtures of {85% A, 5% C, 5% G, 5% T}, {5% A, 85% C, 5% G, 5% T}, {5% A, 5% C, 85% G, 5% T} and {5% A, 5% C, 5% G, 85% T}, respectively.

Next, 0.5 nmol of the oligonucleotide pool (~3×10^{14} molecules) was amplified in a 1-ml PCR reaction for eight cycles by using the forward primer (Primer A: 5′-TCTAATACGACTCACTATA GGAGCTCAGCCTTCACTGC-3′) and reverse primer (Primer B: 5′-GTGGATCCGACCGTGGTGCC-3′) to yield the double-stranded DNA template for the transcription of the library. After phenol:chloroform:isoamyl alcohol (25:24:1, pH 8) extraction, the PCR product was precipitated with sodium acetate and ethanol. The DNA pellet was dissolved in water and directly used for the in vitro transcription reaction.

SELEX. For the first round of selection, a large-scale in vitro transcription mixture (1 ml) containing double-stranded DNA template (0.5 µM), transcription buffer (40 mM Tris pH 8.1, 2 mM spermidine, 22 mM $MgCl_2$, 0.01% Triton X-100), DTT (10 mM), BSA (0.01 mg ml^{-1}), NTP (4 mM each of ATP, CTP, GTP and UTP) and T7 RNA polymerase (1 µM, lab-prepared stock) was prepared. After incubation for 4 h at 37 °C, DNaseI (50 U) was added into the mixture and incubated for 30 min at 37 °C. RNA was purified on a 10% denaturing polyacrylamide gel, excised from the gel and eluted into 0.3 M sodium acetate buffer (pH 5.5) overnight. RNA was precipitated by adding isopropanol and then dissolved in water. To promote the correct folding of the aptamer, the RNA solution was incubated at 75 °C for 2 min and slowly cooled to 25 °C over 10 min. Then, 1/5 volume of 6× aptamer selection buffer (ASB) containing 120 mM HEPES (pH 7.4), 30 mM $MgCl_2$ and 750 mM KCl was added, and the RNA library was incubated at 25 °C for another 10 min.

TMR-decorated beads were prepared by mixing TMR-SS-Biotin (dissolved in water) with streptavidin beads (0.2 ml) in 1× ASB. After 5 min, TMR beads were washed with 1× ASB to remove excess, unbound TMR-SS-Biotin (if any). Next, the folded RNA was mixed with the TMR beads and shaken for 1 h at 25 °C. To remove unbound and low-affinity aptamers, the resin was washed with seven volumes of 1× ASB, and the TMR-bound RNA was eluted with 20 mM DTT, which cleaves the disulfide bond between TMR and biotin. The eluted RNA was ethanol precipitated with glycogen (20 µg), reverse transcribed using SuperScript III (Invitrogen) and PCR amplified for ten cycles. The purified double-stranded DNA template was subjected to the next round of selection. Seven rounds of SELEX were performed using the described protocol with progressively increased stringency. The TMR concentration on the streptavidin resin was decreased from 40 µM (round 1) to 10 µM (rounds 2–7), and the RNA concentration was decreased from 20 µM (round 1) to 10 µM (rounds 2–4) and 5 µM (rounds 5–7), whereas the number of washes to remove low-affinity binders from the resin was increased to 14 volumes of 1× ASB in the final round. After each round of SELEX, the efficiency of the selection was monitored by quantifying the amount of eluted RNA and measuring the fluorescence enhancements of TMR-DN (25 nM) upon addition of the RNA pool (500 nM). After seven rounds, the double-stranded DNA was cloned into a vector, which was subsequently transformed into bacteria, and 96 individual colonies were sent for Sanger sequencing.

Screening of SRB-2 mutants for fluorescence enhancement. Before fluorescence measurements, SRB-2 mutants (1.2 µM, dissolved in water) were incubated at 75 °C for 2 min and then cooled to 25 °C within 10 min to promote the correct folding of the aptamer. Then, 1/5 volume of 6× ASB was added, and the aptamer solution was incubated at 25 °C for an additional 10 min. The fluorescence intensity of the aptamer solutions after addition of TMR-DN (20 nM) was recorded and divided by the fluorescence of TMR-DN without any aptamer to yield fluorescence enhancement values of each mutant. The best mutants were further characterized in detail.

In vitro characterization of SRB aptamers. Aptamers were always folded as described above, and all properties were measured in 20 mM HEPES (pH 7.4), 125 mM KCl and 1 mM $MgCl_2$ buffer unless specified. For fluorescence measurements, excitation and detection wavelengths were set to the excitation and emission maxima of the aptamer:TMR-DN complexes. The fluorescence turn-on value is defined as the ratio of the emission peak intensity of the fluorophore (20 nM) in the presence (500 nM) and absence of SRB aptamers.

Equilibrium dissociation coefficients (K_D) of aptamer:TMR-DN complexes in solution were determined by measuring the fluorescence intensity as a function of RNA concentration in the presence of a fixed amount of TMR-DN (1 nM) at 25 °C. Dissociation coefficients were calculated by fitting the curves to Eq. (1) by using least-squared fitting (OriginPro 8.5.1):

$$F = F_0 + \frac{(F_\infty - F_0) \times \left\{ (K_D + P_0 + [\mathrm{Apt}]) - \sqrt{([\mathrm{Apt}] - P_0)^2 + K_D \times (K_D + 2[\mathrm{Apt}] + 2P_0)} \right\}}{2P_0}, \quad (1)$$

where F is the fluorescence at any given aptamer concentration, F_0 is the fluorescence of the free TMR-DN with initial concentration of P_0, F_∞ is the maximum fluorescence intensity reached when all TMR-DN is in complex with the aptamer, [Apt] is the final concentration of added aptamer, and K_D is the equilibrium dissociation constant.

To determine the Mg^{2+} dependence, 1/5 volume of 6× ASB buffer containing different amounts of $MgCl_2$ (0–10 mM) was added to the RNA (600 nM in water, already incubated at 75 °C for 2 min and cooled to 25 °C) and incubated for 10 min at 25 °C.

To determine the dependence of the aptamer:TMR-DN fluorescence on monovalent cations (Li^+, Na^+, K^+), 1/5 volume of a 6× buffer containing 750 mM of the corresponding cation as chloride salt or without any monovalent cation, 120 mM HEPES (pH 7.4) and 6 mM $MgCl_2$ was added to the aptamer solutions (600 nM in water, already incubated at 75 °C for 2 min and cooled to 25 °C) and incubated for 10 min at 25 °C. Fluorescence intensities were measured upon addition of TMR-DN (500 nM).

To study the temperature dependence of the aptamer:TMR-DN complexes, folded aptamers (500 nM) were incubated with TMR-DN (500 nM) for 10 min. Then, the fluorescence was recorded while increasing the temperature from 25 °C to 65 °C (0.5 °C per minute).

To obtain CD spectra, aptamers (5 µM) were folded in 20 mM Na_2HPO_4/NaH_2PO_4 (pH 7.2), 125 mM KCl and 1 mM $MgCl_2$ as described above and incubated at 25 °C for 10 min. Measurements were performed at 25 °C with 1-nm resolution using a 1-mm cell. CD melting curves of the aptamers (5 µM) were recorded upon increasing the temperature from 25 °C to 98 °C (2 °C per minute) by monitoring the amplitude at 268 nm.

The folding assay was carried out using a slightly modified procedure of Strack et al. [21]. Briefly, the fluorescence intensity of a mixture containing 500 nM aptamer (ten-fold excess) and 50 nM TMR-DN was measured (F_1), so that the amount of formed complex was controlled by the limiting component TMR-DN. Next, the fluorescence intensity of a mixture containing 50 nM aptamer and 500 nM TMR-DN (ten-fold excess) was measured (F_2), where the amount of formed complex is controlled by the limiting component aptamer. Finally, the fluorescence intensity of 500 nM TMR-DN was measured (F_3) for fluorescence background correction due to unbound excess TMR-DN. Fluorescence intensities were measured in 20 mM HEPES (pH 7.4), 1 mM $MgCl_2$ and 125 mM KCl at 25 °C. The fraction of correctly folded aptamer (f) was calculated by using Eq. (2):

$$f = \frac{F_2 - F_3}{F_1 - 0.1F_3}. \quad (2)$$

Quantum yields (QYs) of the aptamer:TMR-DN complexes were determined using a cross-calibrated sulforhodamine 101 standard (QY = 1.00 in ethanol). The integral of the fluorescence emission spectra and the absorbance of the samples at the excitation wavelength (528 nm) were measured for at least four different concentrations of the compounds. To avoid inner filter effects in the fluorescence measurements, concentrations with an absorbance below 0.05 were used. The obtained values were plotted in a graph (integrated fluorescence versus

absorbance). The slope of the linear fit was compared with that of the reference sample, and the QYs were determined using Eq. (3):

$$\mathrm{QY} = \mathrm{QY_R}\left(\frac{m}{m_\mathrm{R}}\right)\left(\frac{n^2}{n_\mathrm{R}^2}\right), \quad (3)$$

where m is the slope, n is the refractive index of the solvent and the subscript R refers to the reference fluorophore with known QY.

For photo-induced fluorescence intensity decay experiments, the JF_{549}-HaloTag ligand[22], the fluorescent protein mRuby3 (ref. [23]), Pepper:HBC620 (ref. [5]) and RhoBAST:TMR-DN were prepared in ASB supplemented with 0.05% (v/v) Tween 20 at a final concentration of 20 nM. RhoBAST:TMR-DN and Pepper:HBC620 (ref. [5]) complexes were freshly prepared by mixing 500 nM of in vitro transcribed RNA and 20 nM of the corresponding dye. All samples were incubated for 30 min at room temperature before the start of the measurement. The samples were irradiated by using an LED setup equipped with a Luxeon Rebel ES Lime LED (nominal wavelength = 567 nm, U = 3.0 V, I = 800 mA). The LED beam illuminated the whole sample ($5\times3\times10\ \mathrm{mm^3}$) in an airtight sealed quartz cuvette. The power of the focused LED beam illuminating the sample volume was determined to be 10.2 mW (680 μW $\mathrm{mm^{-2}}$). All samples were irradiated for 3 h at 25 °C, and the fluorescence of the samples was measured every 20 min.

The kinetics of TMR-DN binding to RhoBAST were investigated using stopped-flow spectroscopy. TMR-DN (5 nM) was titrated with various concentrations of RhoBAST, and the fluorescence intensity at the emission peak was measured over time at 25 °C. Kinetic experiments were performed in either single-molecule (SM) buffer (20 mM HEPES, pH 7.4, 1 mM $MgCl_2$, 125 mM KCl, 0.1% (v/v) Tween 20, 10% (w/w) glucose,1 mM Trolox) or ASB supplemented with 0.05% (v/v) Tween 20. Owing to its slow binding kinetics, the Pepper620 system was studied on the spectrofluorometer by rapid mixing of dye and aptamer.

To extract the apparent rate coefficient, k_{app}, the time-dependent fluorescence, $F(t)$, was fitted using

$$F(t) = (F_0 - F_\infty)e^{-k_{app}t} + F_\infty \quad (4)$$

where F_0 is the initial and F_∞ is the final (equilibrium) fluorescence intensity. The association and dissociation rate coefficients, k_a and k_d, respectively, were obtained by fitting the dependence of k_{app} on the aptamer concentration, [Apt], using

$$k_{app} = k_a[\mathrm{Apt}] + k_d. \quad (5)$$

DNA cloning. For bacterial expression, double-stranded DNA carrying SRB-2, SRB-3, RhoBAST and Pepper sequences (Supplementary Table 3) flanked by EcoRI and SalI restriction sites were created in a PCR reaction, double digested and ligated into EcoRI/SalI double-digested pET-GFP plasmid (Addgene, plasmid no. 29663) to form pET-GFP-SRB-2, pET-GFP-SRB-3, pET-GFP-RhoBAST and pET-GFP-Pepper plasmids. The chloramphenycol acetyl transferase (*cat*) gene was PCR amplified from the pLysS plasmid (Thermo Fisher Scientific, isolated from BL21(DE3)pLysS *E. coli*) and cloned into the HindIII and EcoRI sites of pTAC-MAT-Tag2 (Sigma-Aldrich) to yield the pTac-Cat plasmid. A single-stranded, ultramer oligonucleotide containing two repeats of synonymous RhoBAST (Supplementary Table 3) flanked by SalI and XhoI sites was synthesized, PCR amplified and blunt-end ligated into PCR-linearized pTac-Cat to yield pTac-Cat-$RhoBAST_2$. Another ultramer containing two repeats of synonymous RhoBAST flanked by SalI and XhoI sites was synthesized, PCR amplified, double digested with SalI and XhoI and cloned into XhoI-digested and dephosphorylated pTac-Cat-$RhoBAST_2$ to yield pTac-Cat-$RhoBAST_4$. A cassette containing four repeats of RhoBAST was obtained by PCR using pTac-Cat-$RhoBAST_4$ as a template. $RhoBAST_4$ was then double digested with SalI and XhoI and cloned into XhoI-digested and dephosphorylated pTac-Cat-$RhoBAST_4$ to yield pTac-Cat-$RhoBAST_8$. A cassette containing eight repeats of RhoBAST was obtained by SalI and XhoI double digestion of pTac-Cat-$RhoBAST_8$ followed by gel purification. Cloning this cassette into XhoI-digested and dephosprylated pTac-Cat-$RhoBAST_8$ yielded pTac-Cat-$RhoBAST_{16}$.

The GFP gene carrying HindIII at 5′ and SalI-SphI at 3′ was PCR amplified from the pET-GFP plasmid and cloned into HindIII and SphI sites of pTAC-MAT-Tag2 to yield pTac-GFP. A cassette containing 16 repeats of RhoBAST was obtained by double digestion and gel purification of pTac-Cat-$RhoBAST_{16}$. It was cloned into SalI-digested and dephosphorylated pTac-GFP to yield pTac-GFP-$RhoBAST_{16}$. TolB (MKQALRVAFGFLILWASVLHA), DsbA (MKKIWLALAGLVLAFSASA) and PhoA (MKQSTIALALLPLLFTPVTKA) signal peptide sequences were fused to the N-terminus of GFP in pTac-GFP-$RhoBAST_{16}$ by PCR. Then, linearized plasmids were phosphorylated and self-ligated to form pTac-TolB-GFP-$RhoBAST_{16}$, pTac-DsbA-GFP-$RhoBAST_{16}$ and pTac-PhoA-GFP-$RhoBAST_{16}$.

For mammalian expression, an ultramer ssDNA containing two repeats of synonymous RhoBAST was synthesized, PCR amplified and cloned between the SalI and XbaI sites of pAV-U6+27 (Addgene, plasmid no. 25709) to yield pAV-U6+27-$RhoBAST_2$. To generate pAV-Tornado-RhoBAST, an ultramer ssDNA containing the RhoBAST sequence embedded into the Tornado system[15] was synthesized, PCR amplified and cloned between the SalI and XbaI sites of pAV-U6+27. pUC19-CAG-GFP was prepared by digesting the GFP gene from the AAVS1-mEGFP (Addgene, plasmid no. 91565) plasmid by using SdaI and NotI and cloning it into PCR-linearized pUC19. A cassette containing $RhoBAST_{16}$ was obtained by SalI and XhoI digestion and gel purification of pTac-Cat-$RhoBAST_{16}$. It was then blunted and cloned into pUC19-CAG-GFP, which had already been digested with the MluI enzyme, blunted and dephosphorylated, to yield pUC19-CAG-GFP-$RhoBAST_{16}$. Blunt-end repaired $RhoBAST_{16}$ was cloned into 5′ UTR CGG 99x FMR1-EGFP (Addgene, plasmid no. 63091), which had already been digested with NotI, blunted and dephosphorylated, to yield 5′ UTR CGG 99x FMR1-EGFP-$RhoBAST_{16}$.

***E. coli* K12 genome editing.** To genomically label *ompA* and *rnaseE* with RhoBAST arrays at the 3′ UTR, double-stranded DNA cassettes containing a left homologous arm, $RhoBAST_{16}$, a terminator, a kanamycin expression system and a right homologous arm sequences were prepared by PCR and ligation reactions (Supplementary Table 4). Furthermore, the double-stranded DNA cassette for insertion of the *cat* gene into the *lacz* locus was prepared by double digestion of pTac-Cat-$RhoBAST_{16}$ plasmid with BamHI and PagI and gel purification of the *cat*-$RhoBAST_{16}$ expression system. It was subsequently ligated to a left homologous arm carrying a synthetic terminator at the 5′ end and to a right homologous arm at the 3′ end (Supplementary Table 4). Red/ET homologous recombination in *E. coli* K12 was established using the double-stranded DNA cassettes prepared as described above and the Quick and Easy *E. coli* Gene Deletion Kit (Gene Bridges) according to the manufacturer's instructions. Selection of bacteria with modified genomes was accomplished in the presence of kanamycin for *ompA* and *rnaseE* or chloramphenicol for *cat*. Successful genome modifications were verified by PCR.

Preparation of 5′-Biotin and 3′-Cy5-labeled RhoBAST. T7 RNA polymerase was added into a transcription mixture containing the double-stranded DNA template (5′- TCTAATACGACTCACTATT**A**GGAACCTCCGCGAAAGCGGTGAAG GAGAGGCGCAAGGTTAACCGCCTCAGGTTCC**AA-3′**; the sequence of the T7 φ2.5 promoter is underlined, 1 μM), ATP (0.5 mM), Biotin-HDAAMP (2 mM), CTP (1 mM), GTP (1 mM), UTP (1 mM), DTT (10 mM), spermidine (2 mM), Tris-HCl (40 mM, pH 8.1), $MgCl_2$ (22 mM), Triton X-100 (0.01%), BSA (40 μg $\mathrm{ml^{-1}}$) and pyrophosphatase (1 U $\mathrm{ml^{-1}}$). After 4 h at 37 °C, the reaction mixture was treated with DNaseI (50 U $\mathrm{ml^{-1}}$) for 30 min at 37 °C. RNA was purified by electrophoresis on a 10% denaturing polyacrylamide gel, excised from the gel, ethanol precipitated and dissolved in water. The percentage of biotinylation (~30%) was determined by a streptavidin shift assay. Next, the 3′ end of Biotin-RhoBAST was further ligated to Cy5 by incubating the RNA (10 μM) with ATP (1 mM), pCp-Cy5 (20 μM) and T4 RNA ligase at 4 °C overnight. RNA was then extracted with phenol:chloroform:isoamyl alcohol (25:24:1, pH 4.5), precipitated with sodium acetate and ethanol, dissolved in water and stored at −20 °C. The percentage of Cy5 labeling (~60%) was calculated from the absorption of the Cy5-labeled RNA (extinction coefficients of Cy5: 250,000 $\mathrm{M^{-1}cm^{-1}}$ at 648 nm and 12,500 $\mathrm{M^{-1}cm^{-1}}$ at 260 nm).

Live cell confocal imaging of bacterial cells. BL21 Star (DE3) competent *E. coli* cells were transformed with either pET-GFP (control plasmid) or pET-GFP-SRB-2, -3 or pET-GFP-RhoBAST plasmids. On the following day, single colonies were picked from LB agar/kanamycin (30 μg $\mathrm{ml^{-1}}$) plates and grown in 5 ml of LB medium containing kanamycin (30 μg $\mathrm{ml^{-1}}$) overnight at 37 °C with shaking at 150 r.p.m. A fresh culture with an OD_{600} of 0.01 was started using the overnight culture as a starter culture in a 50-ml Falcon flask containing 10 ml of LB medium with 30 μg $\mathrm{ml^{-1}}$ of kanamycin. When the OD_{600} was 0.4, IPTG (at the desired concentration, ≤1 mM) was added to the culture, and flasks were shaken for an additional 2–3 h at 37 °C. Then, 200 μl of the culture was removed and spun down, and the bacterial pellet was resuspended in 1 ml of M9 medium. Then, 200 μl of this suspension was transferred into a poly-D-lysine (PDL) coated eight-well glass chamber and incubated at 37 °C for 20 min. Finally, the wells were gently washed twice, and bacteria were incubated with 100 nM of TMR-DN in M9 medium for 20 min at 37 °C before imaging.

Images were taken on a point-scanning confocal microscope with hybrid scanner (galvo/resonant) equipped with a Nikon N Apo ×60 NA 1.4 λs OI (WD 0.14 mm, FOV 0.21 × 0.21 $\mathrm{mm^2}$) objective. A 405-nm laser was used to excite Hoechst 33342 (detection via an emission filter set of 450 ± 25 nm); a 488-nm laser was used to excite GFP (emission filter set of 525 ± 25 nm); and a 561-nm laser was used to excite TMR (emission filter set of 595 ± 25 nm). The laser settings were optimized for each condition. z-stack images were taken with a step size of 250 nm. Images were analyzed by Fiji/ImageJ[24], and background was corrected by subtracting the mean fluorescence intensity of a surface area without attached *E. coli* cells from the whole image. The mean fluorescence intensity was determined from defined areas at the poles of the bacteria.

For imaging GFP mRNA using pTac-GFP (control plasmid), pTac-GFP-$RhoBAST_{16}$, pTac-TolB-GFP-$RhoBAST_{16}$, pTac-DsbA-GFP-$RhoBAST_{16}$ and pTac-PhoA-GFP-$RhoBAST_{16}$ plasmids, DH5α cells were used, and the LB growth medium was supplemented with ampicillin (100 μg $\mathrm{ml^{-1}}$) instead of kanamycin. For imaging *ompA* and *rnaseE* mRNA in *E. coli* K12, LB growth

medium was supplemented with kanamycin (15 μg ml^{-1}). For imaging *cat* mRNA in *E. coli* K12, LB growth medium was supplemented with chloramphenicol (10 μg ml^{-1}).

Confocal imaging of fixed *E. coli* cells. Next, 700 μl of bacteria expressing the ROI fused to RhoBAST in LB or M9 medium (as described above) was quickly mixed with 100 μl of 8% PFA solution and incubated for 10 min at room temperature. Bacteria were then pelleted by centrifugation, washed twice with 1 ml of MgPBS (DPBS containing 1 mM $MgCl_2$), resuspended in 1 ml of MgPBS and stored overnight at 4 °C. On the next day, 200 μl of the culture was transferred into a PDL-coated eight-well glass chamber and incubated at room temperature for 20 min. Finally, the wells were gently washed twice, and bacteria were incubated with 1 μg ml^{-1} of Hoechst 33342 and 50 nM TMR-DN in MgPBS (or M9 medium) at 37 °C for 20 min. Then, the bacteria were imaged at room temperature.

RT–qPCR. Chemically competent DH5α *E. coli* cells (Thermo Fisher Scientific) were transformed with pTac-GFP (negative control) and pTac-GFP-RhoBAST$_{16}$. On the next day, single colonies were picked from the LB agar/ampicillin (100 μg ml^{-1}) plates and grown overnight in 5 ml of LB medium containing ampicillin (100 μg ml^{-1}) at 37 °C with shaking. A fresh culture with an OD_{600} of 0.01 was started using the overnight culture as a starter in a 50-ml conical Falcon flask containing 15 ml of LB medium with 100 μg ml^{-1} of ampicillin. After 3 h (OD_{600} ~0.4), the culture was equally divided into three different Falcon flasks, and different amounts of IPTG (0, 10 μM, 40 μM) were added into each culture flask. Cells were shaken for another 2 h at 37 °C. Then, 2 ml of the cultures was spun down, LB medium was carefully removed and the pellet was resuspended in 450 μl of M9 medium. Then, 400 μl of this mixture was used for total RNA isolation, and 50 μl was used for fixed cell imaging. Total RNA from the bacteria was isolated using RNAzol RT according to the manufacturer's instructions, and the obtained RNA pellet was finally dissolved in 200 μl of water.

Total RNA (20 μl, ~2.6 μg) was subjected to DNaseI (50 U ml^{-1}) treatment in 60 μl of total volume at 37 °C for 1 h. DNaseI was inactivated by adding 4 μl of 50 mM EDTA and incubating at 65 °C for 10 min. Complementary DNA was produced using 5 μl of each RNA sample and SuperScript IV-RT (Invitrogen) according to the manufacturer's instructions. Reverse transcription reactions were diluted ten-fold with water before qPCR, which was performed in a Light Cycler 480 instrument (Roche) using the Brilliant III Ultra-Fast SYBR Green qPCR Mastermix (Agilent). Forward and reverse GFP primers are 5′-TGCTGCTGCCCGACAACCAC-3′ and 5′-CGGTCACGAACTCCAGCAGGAC-3′, respectively. qPCR data were analyzed with the LightCycler 480 software. No-RT and no-template reactions were used as negative controls. All reactions were performed in triplicate on the 20-μl scale. 16S rRNA was used as an internal reference gene. For absolute quantification of RNA copy numbers, a small fragment (~180 nucleotides) of the GFP gene was in vitro transcribed and used as a reference RNA in RT–qPCR.

Confocal imaging of live mammalian cells. HeLa or HEK293T cells were cultured at 37 °C under 5% CO_2 in Dulbecco's Modified Eagle's Medium (with 4.5 g L^{-1} high glucose, 4 mM L-glutamine, 25 mM HEPES and without phenol red) supplemented with 10% FBS, 100 U ml^{-1} of penicillin and 100 μg ml^{-1} of streptomycin. To improve the adherence of HEK293T cells, glass slides were coated with PDL before plating the cells.

For imaging experiments, 3×10^4 cells were seeded overnight in μ-Slide chambered coverslips (Ibidi) with eight wells containing 300 μl of medium each. On the following day, cells were transfected with the appropriate plasmid using the FuGeneHD transfection reagent (Promega) according to the manufacturer's protocol. After 48 h at 37 °C, the medium was exchanged with Leibowitz (L15) medium containing 1 μg ml^{-1} of Hoechst 33342 and 100 nM of TMR-DN. After incubation for 1 h, cells were imaged at 37 °C in a live cell imaging chamber with controlled humidity.

Images were taken as described for bacterial cells, except that z-stack images were taken with a step size of 500 nm. Images were analyzed by Fiji/ImageJ. Background was removed by subtracting the mean fluorescence intensity of a surface area without adherent cells from the whole image.

SIM imaging of bacterial cells. DH5α cells *E. coli* cells were transformed with either pTac-GFP (control plasmid) or pTac-GFP-RhoBAST$_{16}$, pTac-TolB-GFP-RhoBAST$_{16}$ or pTac-PhoA-GFP-RhoBAST$_{16}$ plasmids. On the following day, single colonies were picked from LB agar/ampicillin (100 μg ml^{-1}) plates and grown in 5 ml of LB medium containing ampicillin (100 μg ml^{-1}) overnight at 37 °C with shaking at 150 r.p.m. A fresh culture with an OD_{600} of 0.01 was started using the overnight culture as a starter culture in a 50-ml Falcon flask containing 10 ml of LB medium with 100 μg ml^{-1} of ampicillin. When the OD_{600} was 0.4, IPTG (40 μM) was added to the culture, and flasks were shaken for an additional 2–3 h at 37 °C. Then, 200 μl of the culture was removed, spun down and resuspended in 1 ml of M9 medium. At this point, cells were fixed using PFA (see above) and imaged later. For live cell imaging, 200 μl of this suspension was transferred into a PDL-coated eight-well glass chamber and incubated at 37 °C for 20 min. Finally, the wells were gently washed twice, and bacteria were incubated with 50 nM of TMR-DN in M9 medium at 37 °C. Bacteria were imaged after 20-min incubation at 37 °C.

Images were taken on a Nikon N-SIM system equipped with a total internal reflection fluorescence Apochromat 100×1.49 NA oil immersion objective and an electron-multiplying charge-coupled device (EMCCD) camera with single-molecule sensitivity (iXon3 DU897E; Andor Technology). A 488-nm laser was used to excite GFP (detection via an emission filter set of 520/45 nm); a 561-nm laser was used to excite TMR (emission filter set of 610/60 nm). The laser settings were optimized for each condition. Images were taken sequentially within a small z-stack (step size of 150 nm). Subsequently, image reconstruction was performed with the NIS imaging and image analysis software (Nikon).

Dual-color imaging of RhoBAST-tagged mRNAs labeled with smFISH probes and TMR-DN in bacteria. Single-molecule FISH probes (HuluFISH) for GFP were designed and enzymatically labeled with Atto647N by PixelBiotech (see Supplementary Table 3 for sequences). Bacteria expressing various RhoBAST-tagged GFP constructs were fixed in 1% PFA in MgPBS as described above. Bacteria were then pelleted by centrifugation, washed twice with 1 ml of MgPBS and resuspended in 0.3 ml of water, and 0.7 ml of ethanol was added to permeabilize the cells. After 2 h at room temperature, bacteria were centrifuged, and the supernatant was removed. The bacterial pellet was resuspended in 0.5 ml of HuluWash (2× SSC and 2 M urea) and incubated at room temperature for 10 min. The cell suspension was centrifuged, the HuluWash solution was removed and the bacteria were resuspended in 50 μl of HuluHyb (2× SSC, 2 M urea, 10% dextran sulfate, 5× Denhardt's solution) containing FISH probes. After overnight hybridization at 30 °C, bacteria were washed three times with HuluWash for 30 min at 30 °C. Finally, cells were resuspended in MgPBS, immobilized on a PDL-coated eight-well glass chamber, incubated with 0.5 μg ml^{-1} of Hoechst 33342 and 20 nM of TMR-DN in MgPBS for 30 min at room temperature. Images were taken with the confocal microscope as described.

Imaging of immunostained mammalian cells. Next, 3×10^4 HEK293T cells were seeded overnight in a PDL-coated μ-Slide (chambered coverslip) with eight wells containing 300 μl of medium. On the following day, cells were transfected with pAV-Tornado-RhoBAST plasmid (~200 ng per well) using FuGeneHD transfection reagent (Promega) according to the manufacturer's protocol. After 48 h at 37 °C, the medium was exchanged with 300 μl of L15 medium, and half of the medium was removed. Then, 150 μl of 8% PFA (in DPBS, pH 7.4) was added, and the solution was gently but quickly mixed. After 10 min at room temperature, cells were washed three times with 500 μl of MgPBS. To permeabilize the cells, 400 μl of 0.1% Triton X-100 in MgPBS was added to the wells, and cells were incubated for 15 min at room temperature. Triton X-100 was removed, and the cells were washed three times with 500 μl of MgPBS. Before proceeding to immunostaining, cells were incubated with 500 μl of 2% BSA in MgPBS overnight at 4 °C for blocking. On the next day, the appropriate concentration of primary antibody diluted in 500 μl of 0.1% BSA was added to the cells and incubated for 1–2 h at room temperature. All antibodies used in this study and their dilution factors are listed in Supplementary Table 5. The primary antibody solution was removed from the wells, and the cells were washed three times with 500 μl of MgPBS for 5 min. Then, the appropriate concentration of the Alexa488 fluorophore-labeled secondary antibody diluted in 500 μl of 0.1% BSA was added to the cells and incubated for 1 h at room temperature. Finally, the secondary antibody solution was removed from the wells, and the cells were washed three times with 500 μl of MgPBS for 5 min. Before imaging, the solution was exchanged with MgPBS containing 1 μg ml^{-1} of Hoechst 33342 and 100 nM TMR-DN, and the cells were incubated for 10 min at room temperature. Images were taken as described for live mammalian cells; imaging conditions for Alexa488 were identical to those of GFP.

Dual-color imaging of RhoBAST-tagged mRNAs with smFISH probes and TMR-DN in mammalian cells. HEK293T and HeLa cells were transfected with the appropriate plasmids containing a GFP sequence as described above. To ensure a low expression level, HeLa and HEK293T cells expressing *GFP-RhoBAST$_{16}$* mRNA were fixed with 4% PFA already 12 h after transfection. To induce RNA aggregate formation, HeLa cells expressing *(CGG)$_{99}$-FMR1-GFP-RhoBAST$_{16}$* were fixed with 4% PFA 48 h after transfection. Fixed cells on a PDL-coated eight-well glass chamber were permeabilized with 400 μl of 0.1% Triton X-100 in MgPBS for 30 min at room temperature. Triton X-100 was removed, and cells were washed three times with 500 μl of MgPBS and incubated with HuluWash for 10 min. After removing HuluWash, 120 μl of HuluHyb containing FISH probes was added into each well and left for overnight hybridization at 30 °C in a humidified chamber. Subsequently, cells were washed three times with 500 μl of HuluWash and once with MgPBS for 30 min at 30 °C. Finally, cells were incubated with 0.5 μg ml^{-1} of Hoechst 33342 and 20–50 nM TMR-DN in MgPBS for 30 min at room temperature. Images were taken with the confocal microscope as described.

Northern blot analysis of *GFP* and *GFP-RhoBAST$_{16}$* mRNAs in HeLa cells. Four T25 flasks were seeded with HEK293T cells overnight to obtain 60–70% confluency before transfection. On the following day, one flask was transfected with pUC19-CAG-GFP, two flasks were transfected with

pUC19-CAG-GFP-RhoBAST$_{16}$ using FugeneHD transfection reagent and one flask remained untreated. TMR-DN (100 nM) was added to one of the flasks transfected with pUC19-CAG-GFP-RhoBAST$_{16}$. Twenty-four hours after transfection, cells were briefly washed with DPBS, and total RNA was isolated using RNAzol RT according to the manufacturer's instructions. For northern blot analysis, total RNA (~10 µg each) was separated on a 1% agarose gel prepared in 1× MOPS buffer containing 2% formaldehyde and transferred to a Whatman Nytran SuPerCharge nylon blotting membrane (GE Healthcare) overnight at 4 °C by electroblotting. Next, membranes were UV crosslinked and then prehybridized in 15 ml of ULTRAhyb Ultrasensitive Hybridization Buffer (Life Technologies) for 2 h at 46 °C. A GFP-specific DNA probe and a cocktail of DNA probes targeting synonymous RhoBAST sequences (Supplementary Table 3) were prepared using ^{32}P γ-ATP and T4 polynucleotide kinase. A DNA probe (1.5 nM) specific for the GFP sequence was added to the prehybridized membrane and incubated overnight at 46 °C. The blot was washed twice with wash solution 1 (2 × SSC, 0.1% SDS) for 5 min each and again twice with wash solution 2 (0.25 × SSC, 0.1% SDS) for 15 min each. Membranes were visualized using storage phosphor screens (GE Healthcare) and a Typhoon 9400 imager (GE Healthcare). Then, the GFP-specific probe was stripped off by washing the membrane in 0.1% SDS three times for 15 min at 85 °C. The RNAs were rehybridized to RhoBAST-specific DNA probes, washed and imaged as described above.

Single-molecule studies of RhoBAST binding kinetics. In a home-built total internal reflection fluorescence (TIRF) microscope based on an Axiovert 200 frame (Zeiss)[25], light from a 638-nm laser (MLD 638, Cobolt AB) and a 561-nm laser (Jive, Cobolt AB) is combined via dichroic mirrors. The beams pass through into an acousto-optical tunable filter (AOTFnC-400.650, A-A Opto-Electronic) for precise and fast control of laser intensities (Labview 2018) and are guided into a Pellin–Broca prism located on top of a quartz glass sample slide, where they are totally reflected at the boundary between the sample slide and the aqueous sample solution. Immersion oil ($n = 1.518$, Immersol 518 F, Zeiss) between the prism and the quartz glass sample slide ensures undisturbed guidance of the beams to the boundary layer. Fluorescence emission is collected through a water immersion objective (C-Apochromat 63×/1.2 W Corr M27, Zeiss) and detected by an EMCCD camera (Ixon3 DU-897D, Andor) with a pixel size of 120 × 120 nm^2 (Andor Solis v4.24.30004.0). Residual excitation light entering the detection path is blocked by 561-nm and 635-nm notch filters (Thorlabs).

For sample preparation, 75 × 75 × 1-mm^3 quartz slides (Finkenbeiner, Scientific Glass Blower) were sonicated for 30 min at 60 °C in 1 M KOH twice in succession (with fresh KOH). Afterwards, they were sonicated for 15 min at 60 °C in Millipore water twice in succession (with fresh water). Slides were dried under nitrogen, plasma cleaned for 30 min and incubated overnight in 0.05% (v/v) dichlorodimethylsilane (Sigma-Aldrich) solution in *n*-hexane (VWR). On the following day, the slides were sonicated in *n*-hexane at room temperature for 1 min three times in succession, each time with fresh *n*-hexane. Coverslips (20 × 20 × 0.17 mm^3, Menzel Gläser, Thermo Fisher Scientific) were prepared in essentially the same way, except that plasma cleaning was omitted. Quartz glass slides and coverslips were stored at 4 °C until use.

The quartz slides and coverslips were glued together using two pieces of double-sided adhesive tape, leaving a 3-mm-wide channel in the middle. The channel was filled with 20 µl of a 0.01 mg ml^{-1} neutravidin solution in PBS and incubated for 10 min. Then, the channel was washed with 100 µl of PBS and incubated for 10 min with 100 µl of a 0.1 mg ml^{-1} solution of Lutensol AT50 (BASF SE) in water for surface passivation. The channel was washed again with 100 µl of PBS. The RhoBAST stock solution (20 nM in water) was heated to 75 °C for 2 min and then slowly cooled to room temperature before filling it into the channel to ensure proper aptamer folding. To obtain a sparse surface decoration with aptamers, the Cy5-labeled, biotinylated RhoBAST stock was diluted to a final concentration of 25 pM with 1× ASB. The channel was flushed with 100 µl of this solution and incubated for 10 min. Then, the channel was washed with 100 µl of ASB and filled with 20 µl of imaging buffer containing the TMR-DN dye at the desired concentration, an enzymatic oxygen scavenging system (1.4 mg ml^{-1} of glucose oxidase, 0.03 mg ml^{-1} of catalase, 10% (w/w) glucose), 1 mM Trolox as triplet quencher and 0.1% (v/v) Tween 20 in 1× ASB. The channel was sealed with transparent nail polish, and measurements were started after 10 min of equilibration.

To locate RhoBAST molecules, 100 camera frames (100-ms dwell time) were recorded with 638-nm excitation (7 mW in front of the prism) to excite Cy5 attached to the RhoBAST molecules. Then, the Cy5 was photobleached using high (49-mW) laser power to exclude energy transfer from bound TMR-DN dyes to the Cy5 label in the subsequent measurement. Afterwards, TMR-DN was imaged with 561-nm excitation, taking 18,000 frames (100-ms dwell time) with a laser power between 2 and 7 mW.

Images and time traces were analyzed in a semi-automatic way using our own software written in MATLAB 2019a (MATLAB 9.7.0.1190202 (R2019b); MathWorks, 2018). Aptamer locations were identified as local intensity maxima in the images taken in the Cy5 channel. Only maxima with an intensity of 80% or more of the global maximum were included. The intensities in the TMR-DN channel were integrated within a 5 × 5-pixels window around the aptamer positions for all frames and combined in intensity time traces. From these traces, on times (τ_{on}) and off times (τ_{off}) were analyzed by setting a threshold of 3× the s.d. above the mean background. For each time trace, on- and off-time histograms were fitted with an exponential decay to obtain average τ_{on} and τ_{off} values at a single aptamer position. An error of ± 50 ms was assigned to these values to account for the camera dwell time. Average $<\tau_{on}>$ and $<\tau_{off}>$ values were calculated (for identical TMR-DN concentration) as a weighted average according to the uncertainties in the determination of average τ_{on} and τ_{off} values of individual aptamers. Average rate coefficients of dissociation ($k_d = \langle\tau_{on}\rangle^{-1}$) and association ($k'_a = k_a c = \langle\tau_{off}\rangle^{-1}$) were calculated for each dye concentration. The final k_d was obtained by averaging over all concentrations and k_a by a linear regression to the concentration dependence (Fig. 1i). Data were taken at 1.1, 2.2, 4.5, 6.7 and 9.0 nM TMR-DN on 12 (410), 11 (610), 13 (1,230), 8 (1,000) and 10 (1,730) individual molecules, respectively. The numbers in parentheses denote the total number of on-switching events recorded.

Epifluorescence and SMLM imaging. A home-built widefield microscope based on an Axio Observer Z1 frame (Zeiss) with single-molecule sensitivity was used for SMLM, with small modifications from the design described earlier[26]. Light from a 473-nm laser (Gem 473, Laser Quantum) and a 561-nm laser (Gem 561, Laser Quantum) is combined via dichroic mirrors and passed through an AOTF (AOTFnC-400.650, A-A Opto-Electronic) to ensure precise and fast control of the laser intensities (Labview 2017). Two achromatic lenses with focal lengths of 10 mm and 100 mm (Thorlabs) expand the beam after the AOTF. For wide-field illumination, the beam is focused onto the back focal plane of a high numerical aperture oil immersion objective (α Plan-Apochromat 63×/1.46 Oil Corr M27 TIRF, Zeiss) by a scan lens. Fluorescence emission is collected through the same objective and filtered by a quad-band dichroic mirror (z 405/473/561/640, AHF). After the tube lens, a beam splitter (OptoSplit II, Cairn Research) separates the fluorescence into two color channels, which are imaged side by side on an EMCCD camera (Ixon Ultra X-7759, Andor) with a pixel size of 109 × 109 nm^2 (Andor Solis v4.23.30003.0).

In the SMLM measurements, GFP was excited with the 473-nm laser, and its emission was collected through a 525/45-nm (center/width) filter. Typically, 300 camera frames were collected using continuous illumination with an exposure time of 100 ms each and a laser power of 50 µW. Then, the excitation was swiftly changed to 561 nm by means of the AOTF, and TMR-DN was imaged using a 607/70-nm emission filter. Unless noted otherwise, 5,000–10,000 frames were collected with an exposure time of 100 ms each. The laser power was adjusted in the range 4.9–20.4 mW to achieve temporally well-separated blinking events in different cell regions. All laser powers were measured at the sample. Live cell imaging was carried out at 37 °C and 5% CO_2; fixed samples were imaged at room temperature.

SMLM data analysis. To reduce noise in the GFP channel, all 300 camera frames were averaged by using Fiji/ImageJ software. For registration of the SMLM data in the TMR-DN channel, our own custom-written a-livePALM software was used[10]. The major steps of the algorithm include background estimation and Gaussian noise filtering. Based on the detected background information, regions with local maxima are identified. Their location is precisely determined with the maximum likelihood estimator (MLE) algorithm[27]. The localization precision of SMLM images was calculated as described in ref. [28]. Sample drift was typically corrected by a cross-correlation-based analysis[29]. To this end, a reference image was reconstructed from a sub-stack of 500 frames. The following sub-stack was reconstructed; its drift with respect to the reference frame was determined by cross-correlation and compensated. The combined image was subsequently taken as the new reference image. This procedure was repeated for all sub-stacks of the total image stack. Alternatively, 100-nm fluorescent nanoparticles (TetraSpeck microspheres, T7279, Thermo Fisher Scientific) were sparsely immobilized on the glass slide and used as fiducial markers. Final images were generated with Fiji/ImageJ. Intensity profiles were also analyzed with Fiji/ImageJ using a line width of five pixels.

SMLM imaging of *E. coli* bacteria using RhoBAST. *E. coli* cells (strain DH5α) expressing *gfp* (control), *gfp-RhoBAST*, *gfp-RhoBAST$_{16}$*, *tolB-gfp-RhoBAST$_{16}$*, *dsbA-gfp-RhoBAST$_{16}$* and *phoA-gfp-RhoBAST$_{16}$* were grown without IPTG to keep RNA expression low. Cells were fixed and immobilized on a PDL-coated eight-well glass chamber. Samples were incubated with either 15 nM TMR-DN (*gfp* (control), *gfp-RhoBAST$_{16}$*, *tolB-gfp-RhoBAST$_{16}$*, *dsbA-gfp-RhoBAST$_{16}$* and *phoA-gfp-RhoBAST$_{16}$*) or 1 nM TMR-DN (*gfp-RhoBAST*) in M9 medium for 30 min before imaging.

For *gfp* (control)-, *gfp-RhoBAST$_{16}$*-, *tolB-gfp-RhoBAST$_{16}$*-, *dsbA-gfp-RhoBAST$_{16}$*- and *phoA-gfp-RhoBAST$_{16}$*-expressing bacteria, sample drift during data acquisition was corrected using cross-correlation-based analysis[29]. For *gfp-RhoBAST*-expressing bacteria, fiducial markers were used for drift correction.

Comparison of RhoBAST:TMR-DN and Pepper620 in *E. coli* imaging. *E. coli* DH5α cells expressing *gfp-RhoBAST* or *gfp-Pepper* were fixed and immobilized on a cover glass. Then, the bacteria were incubated for 30 min in L15 medium

containing 10 nM of TMR-DN or HBC620, respectively. To quantify the fluorescence decay during imaging, 300 camera frames (100 ms each) were taken in sequence under continuous 561-nm laser illumination at 1.7 mW. In six or seven cellular regions, mean fluorescence intensities were determined for all 300 frames. Background was removed by subtracting the mean fluorescence of ten cells not expressing RhoBAST or Pepper, imaged under identical conditions. All mean intensities were divided by the one of the first frame for normalization and plotted as a function of time.

For a performance comparison of RhoBAST and Pepper in SMLM, fixed bacteria were incubated for 30 min in L15 medium containing TMR-DN or HBC620 at a concentration of 1 nM and then imaged. GFP was imaged as described. TMR-DN and HBC620 were excited at 561 nm (1.7 mW). Then, 14,000 frames (100 ms each) were collected and analyzed; sample drift was compensated by using fiducials.

The performance differences of RhoBAST:TMR-DN and Pepper620 markers in SMLM were visualized by splitting the 14,000 frames into seven bins of 2,000 frames each. For each bin, an SMLM image was reconstructed. The molecule localizations per bin, as detected by the algorithm, were counted. They reveal the differences in dye exchange rates of the two systems. Additionally, Pearson's correlation coefficients between the SMLM image of the first bin (frames 1–2,000) and the reconstructed images of all other bins were determined using Fiji/ImageJ.

SMLM imaging of mammalian cells. HEK293T cells expressing Tornado-RhoBAST were prepared as described. For imaging live cells, the medium was exchanged 48 h after transfection by L15 medium containing 100 nM TMR-DN. After incubation for 1 h, cells were imaged in a live cell imaging chamber. Then, 1,000 frames of TMR-DN were collected with an exposure time of 30 ms each (561-nm excitation, 3.1 mW).

Fixed cells were incubated in DPBS medium containing either 10 nM or 20 nM TMR-DN and 1 mM $MgCl_2$. After incubation for 1 h, 5,000 frames were collected with camera dwell times between 15 ms and 50 ms and excitation laser powers between 3.1 mW and 14.6 mW. Data were analyzed with the a-livePALM software without drift correction. Intensity profiles were analyzed at corresponding positions in the epifluorescence and SMLM images.

Fixed HeLa cells expressing the trinucleotide CGG repeat-containing *FMR1-GFP* mRNA fused to $RhoBAST_{16}$ were incubated in L15 medium containing 10 nM TMR-DN for 30 min before imaging. Hoechst and GFP were excited one after the other using 405-nm and 473-nm light, respectively; their emission was collected through a 525/45-nm filter. 300 camera frames (30 ms each) were collected under continuous illumination (laser power 50–100 µW). Afterwards, 20,000 frames (30 ms each) of TMR emission were collected at an excitation laser power of 20.4 mW. For the three-dimensional (3D) image stack, 5,000 frames each were acquired sequentially at different *Z*-positions. Data were analyzed with the a-livePALM software; sample drift was corrected by cross-correlation-based analysis. Images were created using Fiji/imageJ. The 3D representation in Supplementary Fig. 21c and Supplementary Video 2 were generated with 3D Slicer[30].

For comparison of RhoBAST:TMR-DN localization with smFISH, HeLa cells expressing *GFP-*$RhoBAST_{16}$ mRNA were fixed, permeabilized and hybridized to Atto647N-conjugated smFISH probes (specific to the GFP sequence). Before imaging, the samples were incubated for 30 min in L15 medium containing 10 nM TMR-DN. Atto647N was excited at 640 nm with a laser power of 1.3 mW; the emission was collected through a 684/24-nm filter. 300 frames (100 ms each) were collected using continuous illumination and averaged by using Fiji/ImageJ. Background was cleared with a wavelet-based algorithm. Next, TMR-DN was imaged using a 583/22-nm emission filter. 10,000 frames were collected at a laser power of 20.4 mW. Finally, GFP was excited at 473 nm (100 µW), and the emission was detected through a 583/22-nm emission filter.

Statistical analysis. All data are shown as means ± s.d. with sample size (*n*) listed for each experiment. Statistical analyses were carried out using Prism (GraphPad), OriginPro and Excel (Microsoft). Two-tailed Student's *t*-tests were used to analyze significant differences among SRB-2, SRB-3 and RhoBAST, and the exact *P* values were reported.

Reporting Summary. Further information on research design is available in the Nature Research Reporting Summary linked to this article.

Data availability

The data that support the findings of this study are available upon reasonable request from the corresponding authors. Aptamer sequences used for imaging ROIs are available in the Supplementary Information.

References

21. Strack, R. L., Disney, M. D. & Jaffrey, S. R. *Nat. Methods* **10**, 1219–1224 (2013).
22. Grimm, J. B. et al. *Nat. Methods* **14**, 987–994 (2017).
23. Bajar, B. T. et al. *Sci. Rep.* **6**, 20889 (2016).
24. Schindelin, J. et al. *Nat. Methods* **9**, 676–682 (2012).
25. Manz, C. et al. *Nat. Chem. Biol.* **13**, 1172–1178 (2017).
26. Li, Y., Shang, L. & Nienhaus, G. U. *Nanoscale* **8**, 7423–7429 (2016).
27. Ober, R. J., Ram, S. & Ward, E. S. *Biophys. J.* **86**, 1185–1200 (2004).
28. Deschout, H. et al. *Nat. Methods* **11**, 253–266 (2014).
29. Guizar-Sicairos, M., Thurman, S. T. & Fienup, J. R. *Opt. Lett.* **33**, 156–158 (2008).
30. Fedorov, A. et al. *Magn. Reson. Imaging* **30**, 1323–1341 (2012).

Acknowledgements

M.S. and A.J. were supported by the Deutsche Forschungsgemeinschaft (DFG grant no. Ja794/11) and G.U.N. by the Helmholtz Association (Program Science and Technology of Nanosystems) and the DFG (GRK 2039). We thank the Nikon Imaging Center, Heidelberg for granting access to their facilities, U. Engel for technical advice in fluorescence microscopy and M. Mayer and L. Rohland for assistance with stopped-flow measurements. We gratefully acknowledge R. Ma and A. Kobitski for technical support with SMLM experiments and analysis. We thank BASF SE for kindly providing Lutensol AT50.

Author contributions

M.S., G.U.N. and A.J. designed the study. A.M. and M.S. evolved RhoBAST, and M.S., D.E. and F.G. characterized RhoBAST's photophysical properties. M.S. created all plasmid constructs and strains and carried out confocal and SIM microscopy. J.L. carried out SMLM experiments and analyzed the data. J.L. and B.H. developed the assay for single-molecule binding kinetics and performed the experiments and analysis. M.S., K.N., G.U.N. and A.J. supervised the work. M.S. wrote the first draft, and all authors contributed to reviewing, editing and providing additional text for the manuscript.

Competing interests

The authors declare no competing interests.

Additional information

Supplementary information The online version contains supplementary material available at https://doi.org/10.1038/s41587-020-00794-3.

Correspondence and requests for materials should be addressed to M.S., G.U.N. or A.J.

Peer review information *Nature Biotechnology* thanks Don Lamb and the other, anonymous, reviewer(s) for their contribution to the peer review of this work.

Reprints and permissions information is available at www.nature.com/reprints.

nature research

Corresponding author(s): Murat Sunbul, G. Ulrich Nienhaus, Andres Jäschke

Last updated by author(s): Nov 24, 2020

Reporting Summary

Nature Research wishes to improve the reproducibility of the work that we publish. This form provides structure for consistency and transparency in reporting. For further information on Nature Research policies, see Authors & Referees and the Editorial Policy Checklist.

Statistics

For all statistical analyses, confirm that the following items are present in the figure legend, table legend, main text, or Methods section.

n/a	Confirmed	
☐	☒	The exact sample size (*n*) for each experimental group/condition, given as a discrete number and unit of measurement
☐	☒	A statement on whether measurements were taken from distinct samples or whether the same sample was measured repeatedly
☐	☒	The statistical test(s) used AND whether they are one- or two-sided *Only common tests should be described solely by name; describe more complex techniques in the Methods section.*
☒	☐	A description of all covariates tested
☒	☐	A description of any assumptions or corrections, such as tests of normality and adjustment for multiple comparisons
☐	☒	A full description of the statistical parameters including central tendency (e.g. means) or other basic estimates (e.g. regression coefficient) AND variation (e.g. standard deviation) or associated estimates of uncertainty (e.g. confidence intervals)
☐	☒	For null hypothesis testing, the test statistic (e.g. *F*, *t*, *r*) with confidence intervals, effect sizes, degrees of freedom and *P* value noted *Give P values as exact values whenever suitable.*
☒	☐	For Bayesian analysis, information on the choice of priors and Markov chain Monte Carlo settings
☒	☐	For hierarchical and complex designs, identification of the appropriate level for tests and full reporting of outcomes
☐	☒	Estimates of effect sizes (e.g. Cohen's *d*, Pearson's *r*), indicating how they were calculated

Our web collection on statistics for biologists contains articles on many of the points above.

Software and code

Policy information about availability of computer code

Data collection	Nikon A1R confocal microscope, Nikon N-SIM super-resolution microscope, Andor Solis (version 4.23.30003.0 and 4.24.30004.0) for SMLM image acquisition, custom-written software in Labview 2018 and Labview 2017 for control of the microscope setups.
Data analysis	ImageJ (1.51s), OriginPro (2015), custom-written software in MATLAB (2019b), GraphPad Prism 6, NIS-Elements C to construct SIM images, LightCycler 480 software for qPCR analysis, Microsoft Excel 2016 MSO.

For manuscripts utilizing custom algorithms or software that are central to the research but not yet described in published literature, software must be made available to editors/reviewers. We strongly encourage code deposition in a community repository (e.g. GitHub). See the Nature Research guidelines for submitting code & software for further information.

Data

Policy information about availability of data

All manuscripts must include a data availability statement. This statement should provide the following information, where applicable:

- Accession codes, unique identifiers, or web links for publicly available datasets
- A list of figures that have associated raw data
- A description of any restrictions on data availability

The data that support the findings of this study are available upon reasonable request from the corresponding authors. Aptamer sequences used for imaging ROIs are available in the Supplementary Information .

Field-specific reporting

Please select the one below that is the best fit for your research. If you are not sure, read the appropriate sections before making your selection.

☒ Life sciences ☐ Behavioural & social sciences ☐ Ecological, evolutionary & environmental sciences

For a reference copy of the document with all sections, see nature.com/documents/nr-reporting-summary-flat.pdf

Life sciences study design

All studies must disclose on these points even when the disclosure is negative.

Sample size	The sample size of each experiment was given in the corresponding figure legend where applicable. The selected sample sizes were sufficiently powered to validate statistical differences in mean values of the investigated parameters. No statistical method was used to predetermine the sample-size. All imaging experiments were carried out in at least three different cell cultures (unless otherwise noted), giving reproducible and consistent results about the RNA localizations and expression levels.
Data exclusions	No data was excluded from the analysis.
Replication	The replication number was reported in the figure legend of the corresponding data where applicable. For in vitro characterization of RhoBAST, at least three independent experiments, and for SMLM, SIM or confocal microscopy of cells, at least three independent experiments were carried out with similar results. All replicates were successful.
Randomization	No randomization was performed due to the nature of the experiments.
Blinding	No blinding was performed due to the nature of the experiments.

Reporting for specific materials, systems and methods

We require information from authors about some types of materials, experimental systems and methods used in many studies. Here, indicate whether each material, system or method listed is relevant to your study. If you are not sure if a list item applies to your research, read the appropriate section before selecting a response.

Materials & experimental systems

n/a	Involved in the study
☐	☒ Antibodies
☐	☒ Eukaryotic cell lines
☒	☐ Palaeontology
☒	☐ Animals and other organisms
☒	☐ Human research participants
☒	☐ Clinical data

Methods

n/a	Involved in the study
☒	☐ ChIP-seq
☒	☐ Flow cytometry
☒	☐ MRI-based neuroimaging

Antibodies

Antibodies used	Anti-Nucleolin (Rabbit, Thermo Fisher, PA5-82860), Anti-NPM1 (Mouse, Thermo Fisher, 32-5200), Anti-Fibrillarin (Mouse, Thermo Fisher, 480009), Anti-RTCB (Rabbit, Thermo Fisher, PA5-64867), Anti-NONO (Rabbit, Sigma Aldrich, N8789), Anti-PSPC1 (Rabbit, Thermo Fisher, PA5-58585), Anti-Sam68 (Rabbit, Sigma Aldrich, HPA051280), Anti-NPAT (Rabbit, Thermo Fisher, PA5-66839), Anti-POLR3B (Rabbit, Thermo Fisher, PA5-57671), Anti-Coilin (Mouse, Sigma Aldrich, C1862), Anti-SC35 (Mouse, Sigma Aldrich, S4045), Anti-IRS1 (Rabbit, Thermo Fisher, PA1-1057), Anti-Mouse IgG Alexa488 (Goat, Thermo Fisher, A28175), Anti-Rabbit IgG Alexa488 (Goat, Thermo Fisher, A11008)
Validation	All antibodies used in this study were validated by the manufacturers (Sigma-Aldrich and Thermo Fisher Scientific). More information can be found on the manufacturer's website: 1) Anti-Nucleolin (Rabbit, Thermo Fisher, PA5-82860), https://www.thermofisher.com/antibody/product/Nucleolin-Antibody-Polyclonal/PA5-82860 2) Anti-NPM1 (Mouse, Thermo Fisher, 32-5200), https://www.thermofisher.com/antibody/product/NPM1-Antibody-clone-FC-61991-Monoclonal/32-5200 3) Anti-Fibrillarin (Mouse, Thermo Fisher, 480009), https://www.thermofisher.com/antibody/product/Fibrillarin-Antibody-clone-38F3-Monoclonal/480009 4) Anti-RTCB (Rabbit, Thermo Fisher, PA5-64867), https://www.thermofisher.com/antibody/product/RTCB-Antibody-Polyclonal/PA5-64867 5) Anti-NONO (Rabbit, Sigma Aldrich, N8789), https://www.sigmaaldrich.com/catalog/product/sigma/n8789?lang=de&region=DE 6) Anti-PSPC1 (Rabbit, Thermo Fisher, PA5-58585), https://www.thermofisher.com/antibody/product/PSPC1-Antibody-Polyclonal/PA5-58585 7) Anti-Sam68 (Rabbit, Sigma Aldrich, HPA051280), https://www.sigmaaldrich.com/catalog/product/sigma/hpa051280?

lang=de&region=DE
8) Anti-NPAT (Rabbit, Thermo Fisher, PA5-66839), https://www.thermofisher.com/antibody/product/NPAT-Antibody-Polyclonal/PA5-66839
9) Anti-POLR3B (Rabbit, Thermo Fisher, PA5-57671), https://www.thermofisher.com/antibody/product/POLR3B-Antibody-Polyclonal/PA5-57671
10) Anti-Coilin (Mouse, Sigma Aldrich, C1862), https://www.sigmaaldrich.com/catalog/product/sigma/c1862?lang=de&region=DE
11) Anti-SC35 (Mouse, Sigma Aldrich, S4045), https://www.sigmaaldrich.com/catalog/product/sigma/s4045?lang=de&region=DE
12) Anti-IRS1 (Rabbit, Thermo Fisher, PA1-1057), https://www.thermofisher.com/antibody/product/IRS1-Antibody-Polyclonal/PA1-1057
13) Anti-Mouse IgG Alexa488 (Goat, Thermo Fisher, A28175), https://www.thermofisher.com/antibody/product/Goat-anti-Mouse-IgG-H-L-Secondary-Antibody-Recombinant-Polyclonal/A28175
14) Anti-Rabbit IgG Alexa488 (Goat, Thermo Fisher, A11008), https://www.thermofisher.com/antibody/product/Goat-anti-Rabbit-IgG-H-L-Cross-Adsorbed-Secondary-Antibody-Polyclonal/A-11008

Eukaryotic cell lines

Policy information about cell lines

Cell line source(s)	HEK293T (ACC 635) and HeLa (ACC 57) cells were obtained from DSMZ.
Authentication	Cell lines were not authenticated.
Mycoplasma contamination	Cell lines were not tested for mycoplasma.
Commonly misidentified lines (See ICLAC register)	No commonly misidentified cell lines were used.